JACS
JOURNAL OF THE AMERICAN CHEMICAL SOCIETY

Communication

pubs.acs.org/JACS

Fluorogenic, Two-Photon-Triggered Photoclick Chemistry in Live Mammalian Cells

Zhipeng Yu,[†] Tymish Y. Ohulchanskyy,[‡] Peng An,[†] Paras N. Prasad,[‡] and Qing Lin*[,†]

[†]Department of Chemistry, State University of New York at Buffalo, Buffalo, New York 14260, United States

[‡]Institute for Lasers, Photonics and Biophotonics (ILPB) and Department of Chemistry, State University of New York at Buffalo, Buffalo, New York 14260, United States

Supporting Information

ABSTRACT: The tetrazole-based photoclick chemistry has provided a powerful tool to image proteins in live cells. To extend photoclick chemistry to living organisms with improved spatiotemporal control, here we report the design of naphthalene-based tetrazoles that can be efficiently activated by two-photon excitation with a 700 nm femtosecond pulsed laser. A water-soluble, cell-permeable naphthalene-based tetrazole was identified that reacts with acrylamide with the effective two-photon cross-section for the cycloaddition reaction determined to be 3.8 GM. Furthermore, the use of this naphthalene-tetrazole for real-time, spatially controlled imaging of microtubules in live mammalian cells via the fluorogenic, two-photon-triggered photoclick chemistry was demonstrated.

Compared with single-photon processes, two-photon excitation (2PE) induced processes offer a superior spatiotemporal control due to the reduced scattering of near-infrared (NIR) light in turbid biological tissues and significantly improved three-dimensional localization of excitation.[1] In addition, the use of NIR light provides deeper tissue penetration, utilizing the biological window of maximum optical transparency (~700−1000 nm). The prominent 2PE induced reactions suitable for biological applications included the reversible photochromic reactions for targeted imaging of cancer cells[2] and the photo "uncaging" of caged ligands for regulating physiological function in tissues.[3] For example, the use of 6-bromo-7-hydroxycoumarin-4-ylmethyl (Bhc)-caged glutamate allowed the three-dimensional mapping of the glutamate sensitivity of neurons in intact brain slices.[4] Invariably, the two-photon-sensitive "caging" groups are sacrificed after their release. Here, we report a new 2PE induced chemistry in which a transient, highly reactive 1,3-dipole is generated from the appropriately functionalized tetrazole upon photoirradiation with a femtosecond pulsed laser, and subsequently intercepted by a suitable dipolarophiles via 1,3-dipolar cycloaddition reaction to generate a fluorescent cycloadduct (Figure 1a). We demonstrate that this tetrazole-mediated two-photon-triggered reaction can be employed to image microtubules in real time in a spatiotemporally controlled manner in live mammalian cells.

Our previous work on the photoinduced tetrazole-alkene addition reaction ("photoclick" chemistry) have identified

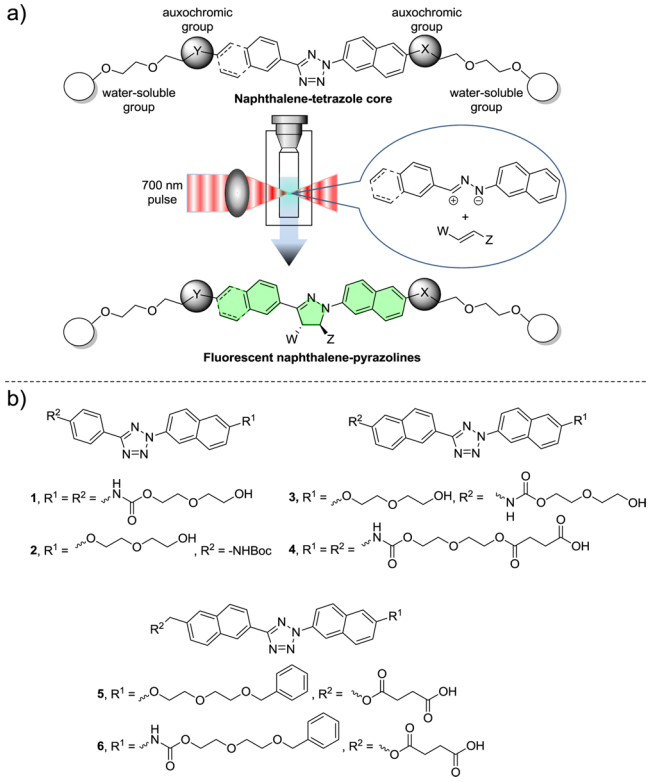

Figure 1. Design of naphthalene-tetrazoles for fluorogenic, two-photon-triggered photoclick chemistry. (a) General features of the naphthalene-tetrazoles and scheme of fluorogenic, two-photon-triggered photoclick chemistry. (b) Chemical structures of the naphthalene-tetrazoles **1**−**6** used in this study.

tetrazoles that can be activated by single-photon UV light.[5] To extend this chemistry to two-photon near-IR activation, we took advantage of the strong two-photon absorption properties of the naphthalene structure[6] and synthesized a series of naphthalene-based tetrazoles **1**−**6** (Figure 1b; Schemes S1−S6, Supporting Information (SI)). Functionalization of naphthalene β-position with the various auxochromic and oligo(ethyleneglycol) groups was expected to fine-tune two-photon absorption properties[7] and increase water-solubility and potential cell-permeability, respectively. The UV−vis spectra

Received: July 30, 2013
Published: October 29, 2013

   dx.doi.org/10.1021/ja407867a | J. Am. Chem. Soc. 2013, 135, 16766−16769

of tetrazoles **1**–**6** were recorded (Figure S1 (SI)), and their absorption characteristics are collected in Table 1. Among them, tetrazole **4** with the longest conjugation system (two naphthalene rings and two carbamates) showed the most bathochromic shift of the absorption peak (λ_{max} = 324 nm) and highest extinction coefficient at 365 nm (Table 1).

Table 1. Photophysical Properties of Tetrazoles and Their Kinetic Constants in the Single-Photon Induced Cycloaddition Reaction[a]

tetrazole	λ_{max}[b] (nm)	ε_{max}[c] (M^{-1} cm^{-1})	ε_{365}[d] (M^{-1} cm^{-1})	k_0[e] (μM s^{-1})	Φ_T[f]
1	322	31 000	1700	0.27	0.33
2	316	24 000	690	0.25	0.75
3	322	40 000	1900	0.048	0.053
4	324	41 000	4500	0.064	0.029
5	314	32 000	1300	0.29	0.47
6	318	32 000	2000	0.33	0.33

[a]Compounds were dissolved in acetonitrile/PBS (1:1) to obtain a concentration of 25 μM. For the cycloaddition reaction, 2.5 mM acrylamide (100 equiv) was used to drive the full conversion of nitrile imine to pyrazoline. [b]λ_{max} in the 300–500 nm region. [c]Extinction coefficient at λ_{max}. [d]Extinction coefficient at 365 nm. [e]Zero-order rate constant under 365 nm photoirradiation. [f]Quantum yield of tetrazole ring rupture under 365 nm photoirradiation.

The photochemical step of this reaction involves light-triggered rupture of the tetrazole ring to generate in situ a highly reactive nitrile imine dipole.[8] To determine the ring-rupture kinetics, we subjected a solution of tetrazole and 100 equiv of acrylamide dipolarophile to photoirradiation with a hand-held 365 nm UV lamp. Plotting the pyrazoline cycloadduct formation in the first 80 s of photoirradiation (when the rate-limiting step is the rupture of the tetrazole ring) gave the zero-order rate constant, k_0, for the various tetrazoles (Figure 2, Table 1). Interestingly, tetrazole **5** showed the second fastest kinetics (k_0 = 0.29 μM s^{-1}) despite its relatively low extinction coefficient, while tetrazole **4**, with the strongest absorption at 365 nm, showed significantly slower kinetics (k_0 = 0.064 μM s^{-1}). This apparent discrepancy can be explained by their large difference in the quantum yield (Φ_T = 0.47 for **5** vs 0.029 for **4**; Table 1) determined by ferrioxalate-polyoxometalate-based chemical actinometer (Figure S2 (SI)).[9] In a subtle way, tetrazole **6** with the carbamate group on the *N*-naphthalene ring and the naphthylmethyl ester on the *C*-aryl side showed the fastest ring rupture kinetics under 365 nm photoirradiation.

To identify a suitable NIR wavelength for two-photon activation of tetrazoles, we irradiated a solution of tetrazole **1** and 100 equiv of acrylamide in acetonitrile/PBS (1:1) with a tunable fs-pulsed laser with the wavelength set at 750, 730, or 700 nm, and found that 700 nm was most conducive to the cycloadduct formation (Figure S3 (SI)). We then performed the kinetic analysis of the two-photon-triggered cycloaddition reaction for all tetrazoles by following the fluorescence spectra of the newly generated fluorescent pyrazoline cycloadducts (Figures S4–S8 (SI)). As an illustration, Figure 2a shows the absorption change and the fluorescence "turn-on" over time[10] when a solution of tetrazole **6** and acrylamide was irradiated with a 700 nm femtosecond pulsed laser. A plot of the time course of the cycloadduct formation revealed that the two-photon-triggered cycloaddition reaction follows the zero-order kinetics (k_0 = 0.067 ± 0.001 μM/min), indicating that the photoinduced tetrazole ring rupture is the rate-determining step (Figure 2b). By comparing the cycloaddition rate to that of uncaging of BHC acetate (BHC-OAc) (k_0 = 0.0372 ± 0.0044 μM/min, Figure 2c), the effective two-photon cycloaddition cross-section for tetrazole **6** was calculated to be 3.8 GM.[11] Assuming quantum yield of the tetrazole ring-rupture under two-photon activation is the same as under single-photon activation, the two-photon absorption cross-section was then calculated on the basis of the following equation, $\delta_{aT} = \delta_{cT}/\Phi_T$, and the data are collected in Figure 2d. Among the naphthalene-tetrazoles, tetrazole **4** with the longest π conjugation showed the highest absorption cross-section (δ_{aT} = 45 GM). However, its effective two photon cycloaddition cross-section is the lowest (δ_{cT} = 1.3 GM), a result of its extremely low quantum yield (Figure 2d). This large discrepancy between the cycloaddition cross-section and the absorption cross-section reinforces the notion that high quantum yield of the tetrazole ring rupture, an intrinsic property of the excited tetrazole species, is vital to the overall efficiency of the two-photon-triggered photoclick chemistry.

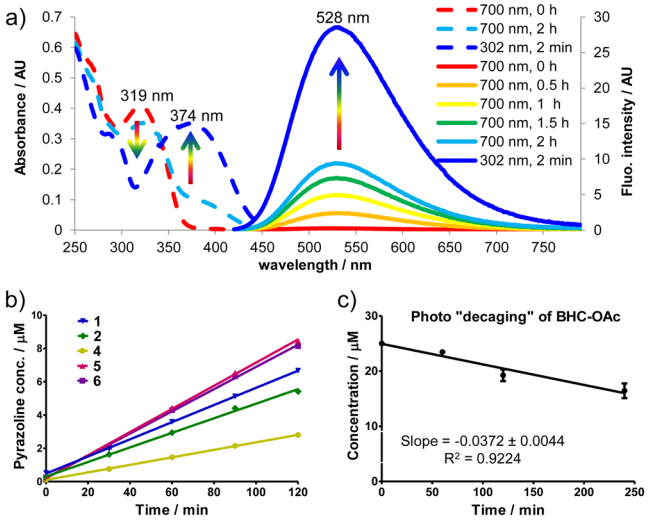

d)

Tetrazole	1	2	4	5	6
k_0 (μM/min)	0.0520 ± 0.0005	0.044 ± 0.001	0.0230 ± 0.0002	0.070 ±0.001	0.067 ± 0.001
Φ_T	0.33	0.75	0.029	0.47	0.33
δ_{cT} (GM)	3.0	2.5	1.3	4.0	3.8
δ_{aT} (GM)	9.1	3.3	45	8.5	12

Figure 2. Determining tetrazole two-photon absorption cross-section and two-photon cycloaddition cross-section. (a) UV–vis (dash line) and fluorescence spectra (solid line) monitoring of the cycloaddition reaction between 25 μM tetrazole **6** and 2.5 mM acrylamide in acetonitrile/PBS (1:1) under 700 nm femtosecond pulsed laser irradiation. For fluorescence measurement, λ_{ex} = 405 nm. (b) Plot of the pyrazoline cycloadduct formation over 120 min of 700 nm femtosecond pulsed laser irradiation. Tetrazole **3** was not included because of its insufficient solubility in acetonitrile/PBS (1:1). (c) Plot of the time course of photodecaging of BHC-OAc upon 740 nm femtosecond pulsed laser irradiation. (d) Kinetic and photophysical data for naphthalene-tetrazoles in the two-photon-triggered photoclick chemistry. The two-photon cross-section of the cycloaddition reaction, δ_{cT}, and two-photon absorption cross-section, δ_{aT}, were measured in GM (10^{-50} cm^4 s/photon).

Since acrylamide has recently been introduced into proteins site-specifically in the form of N^{ε}-acryloyl-L-lysine (AcrK),[12] we examined whether the naphthalene-based tetrazoles can label the AcrK-encoded proteins selectively under the two-photon condition. Two sfGFP mutants, sfGFP-S2BocK and sfGFP-

dx.doi.org/10.1021/ja407867a | J. Am. Chem. Soc. 2013, 135, 16766–16769

S2AcrK, carrying *tert*-butyloxycarbonyl-lysine (BocK) and AcrK at Ser-2 position, respectively, were expressed and purified to homogeneity (Figures S10 and S11 (SI)). We irradiated the solutions of 10 μM of sfGFP-S2AcrK or sfGFP-S2BocK and 200 μM of tetrazole **6** with the 700 nm femtosecond pulsed laser at room temperature for 4 h (Figure 3a). In-gel

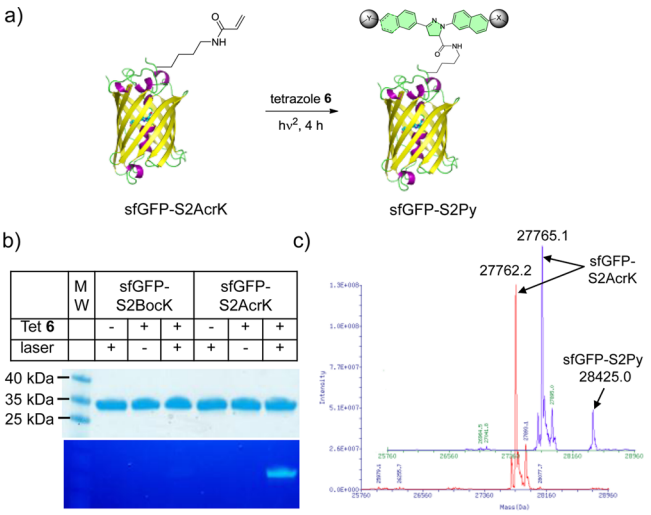

Figure 3. Selective femtosecond pulsed laser induced fluorogenic labeling of sfGFP-S2AcrK by tetrazole **6** in vitro. (a) Reaction scheme. A solution of 10 μM sfGFP-S2AcrK and 200 μM tetrazole **6** in PBS buffer in a quartz cuvette was irradiated with a 700 nm femtosecond laser for 4 h. (b) Coomassie blue stain (top panel) and in-gel fluorescence (bottom panel) of the same protein gel after the reaction mixtures were resolved by SDS-PAGE. (c) Deconvoluted mass spectra of sfGFP-S2AcrK (in red) and the product mixture (in blue) showing the formation of the pyrazoline adduct.

fluorescence analysis of the reaction mixtures after SDS-PAGE showed that the two-photon-triggered photoclick chemistry proceeded nicely with sfGFP-S2AcrK but not with sfGFP-S2BocK (Figure 3b). ESI-MS revealed an intact mass of 28425.0 ± 3.2 Da for the pyrazoline adduct (Figure 3c), matching the theoretic mass of 28425.3 Da, with conversion estimated to be 16.5% (Figure S12 (SI)).

To probe whether the pyrazoline cycloadducts derived from the naphthalene-tetrazoles can be directly monitored in situ using fluorescence microscopy, we tested the ability of tetrazole **6**[13] to fluorescently label microtubules in cultured CHO cells that are pretreated with a fumarate-modified docetaxel under 365 nm photoirradiation condition.[14] To this end, we synthesized a fumarate-docetaxel conjugate, IPFAD, by appending monoisopropyl fumarate amide (IPFA) at position 10 of docetaxel via a flexible linker (Scheme S7 (SI)) on the basis of the following considerations: (i) monoisopropyl fumarate amide (IPFA) is chemically stable toward glutathione, a biological nucleophile present in high concentrations inside living cells (Figure S14 (SI)); (ii) modification at position 10 of docetaxel does not affect the binding of docetaxel to microtubules;[15] and (iii) IPFA gave a fast cycloaddition reaction with tetrazole **6** with the second-order rate constant, k_2, of 89 ± 8.5 M^{-1} s^{-1} (Figure S15 (SI)). Indeed, the IPFAD-treated cells showed significantly higher cytosolic fluorescence after the 365 nm UV triggered photoclick chemistry compared to the untreated cells (Figure S16 (SI)). Spectral scan of the fluorescent cells revealed a hypsochromic shift in emission maximum (λ_{em} = 498 nm) accompanied by an increase in intensity (Figure S16 (SI)), suggesting that the pyrazoline-docetaxel cycloadduct likely binds to a hydrophobic pocket on the microtubules where the dielectric constant is low (Figures S17 and S18 (SI)).[16]

To demonstrate that the naphthalene-tetrazole can mediate two-photon-triggered photoclick chemistry in vivo, we treated CHO cells with 3 μM of tetrazole **6** and 40 μM of IPFAD[17] followed by photoirradiation with a 700 nm femtosecond pulsed laser (<140 fs pulse width, 90 MHz). Specifically, a rectangle area in the culture dish was selected for continuous photoirradiation by the 700 nm femtosecond laser, and the time-lapsed fluorescence images were acquired using a confocal laser scanning microscope (ex, 405 nm; em, 462−580 nm). Only the IPFAD-treated CHO cells showed fast, time-dependent rise in cytosolic fluorescence in the irradiated area[18] (Figure 4a; compare top row to bottom row).

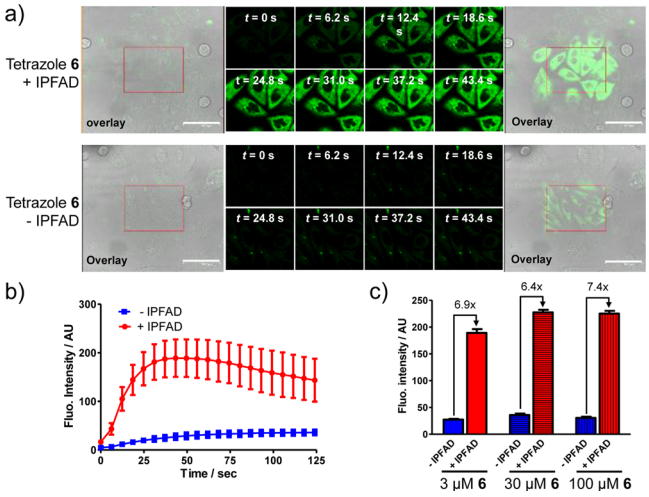

Figure 4. Fluorescence microscopy of the fluorogenic, two-photon-triggered photoclick chemistry in CHO cells. (a) Fluorescence/DIC overlap image before photoirradiation (panel 1), time-lapsed fluorescence images (panels 2−9), and fluorescence/DIC overlap image after photoirradiation (panel 10). CHO cells were treated with 3 μM tetrazole **6** in the presence (top row) or absence (bottom row) of 40 μM IPFAD followed by photoillumination of the red rectangle area with a 700 nm femtosecond pulsed laser. Scale bar = 61.3 μm. (b) Time courses of fluorescence development in 10 cytosolic regions in selected CHO cells; red curve denotes the regions in the IPFAD-treated cells, while blue curve denotes the regions in the untreated cells. The concentrations of tetrazole **6** and IPFAD were 3 and 40 μM, respectively. (c) Effect of tetrazole **6** concentration on fluorescence intensity monitored by confocal microscopy. See Figure S21 (SI) for details.

Quantification of the cytosolic fluorescence indicates that the intensity reached a plateau at about 43 s,[19] while there was a gradual increase in background fluorescence for cells without the IPFAD treatment (Figure 4b), likely due to the photogenerated weakly fluorescent nitrile imine intermediate.[20] Interestingly, increasing tetrazole **6** concentrations led to small increases in fluorescence intensity along with increased background, with the signal-to-background ratio staying about the same (Figure 4c, Figure S21 (SI)), suggesting that the two-photon-triggered tetrazole ring rupture, the rate-determining step of the reaction, is essentially independent of the initial tetrazole concentration. This result is consistent with the in vitro activation studies (Figure 2b). The specificity of

dx.doi.org/10.1021/ja407867a | J. Am. Chem. Soc. 2013, 135, 16766−16769

microtubule labeling was confirmed by two-color overlay[21] in which the microtubules were immunostained using an anti-α-tubulin antibody (Figure S22 (SI)). It is noteworthy that the in situ formed pyrazoline-docetaxel gave higher efficiency in labeling microtubules than treating cells with the preformed pyrazoline-docetaxel at the identical concentration (Figure S23 (SI)), presumably due to poorer permeability of the pyrazoline-docetaxel, indicating a unique advantage for our two-step in situ labeling procedure.

In summary, we have developed a new type of two-photon-triggered chemistry in which the two-photon generated, highly reactive intermediates undergo spontaneous and specific 1,3-dipolar cycloaddition reactions with the suitable dipolarophiles to generate in situ the fluorescent cycloadducts. This naphthalene-tetrazole mediated two-photon reaction showed higher two-photon reaction cross-sections than the two-photon uncaging action cross-sections for commonly used two-photon caging groups.[22] Moreover, the utilities of this two-photon-triggered, fluorogenic photoclick chemistry in labeling an alkene-encoded protein site-selectively in vitro and ligand-bound microtubules in cultured cells were demonstrated. Since the genetic methods to encode the unnatural amino acids containing reactive alkene dipolarophiles have been reported for both cultured mammalian cells[23] and *Drosophila melanogaster* fruit fly,[24] we expect this naphthalene-tetrazole-based two-photon chemistry to offer a new tool to dissect protein function in living organisms with a high spatiotemporal precision.

■ ASSOCIATED CONTENT

Ⓢ Supporting Information

Supplemental figures and table, synthetic schemes, experimental procedures, and characterization of all new compounds. This material is available free of charge via the Internet at http://pubs.acs.org.

■ AUTHOR INFORMATION

Corresponding Author

qinglin@buffalo.edu

Notes

The authors declare no competing financial interest.

■ ACKNOWLEDGMENTS

We gratefully acknowledge the National Institutes of Health (GM 085092) for financial support. We thank Dr. Guang S. He at ILPB for helpful discussions, Alan Siegel at SUNY Buffalo Biological Sciences Imaging Facility (supported by the National Science Foundation Major Research Instrumentation Grant DBI-0923133) for assistance with microscopy, and Dr. Wenshe Liu at Texas A&M University for generously providing us the plasmids pEvol-PylT-PylKRS, pEvol-AcrKRS, and pET-sfGFPS2TAG.

■ REFERENCES

(1) Helmchen, F.; Denk, W. *Nat. Methods* **2005**, *2*, 932−940.

(2) Zhu, M. Q.; Zhang, G. F.; Li, C.; Aldred, M. P.; Chang, E.; Drezek, R. A.; Li, A. D. *J. Am. Chem. Soc.* **2011**, *133*, 365−372.

(3) Bort, G.; Gallavardin, T.; Ogden, D.; Dalko, P. I. *Angew. Chem., Int. Ed.* **2013**, *52*, 4526−4537 and references therein.

(4) Furuta, T.; Wang, S. S.-H.; Dantzker, J. L.; Dore, T. M.; Bybee, W. J.; Callaway, E. M.; Denk, W.; Tsien, R. Y. *Proc. Natl. Acad. Sci. U. S. A.* **1999**, *96*, 1193−1200.

(5) (a) Lim, R. K.; Lin, Q. *Acc. Chem. Res.* **2011**, *44*, 828−839. (b) Wang, Y.; Hu, W. J.; Song, W.; Lim, R. K.; Lin, Q. *Org. Lett.* **2008**, *10*, 3725−3728. (c) Yu, Z.; Ho, L. Y.; Wang, Z.; Lin, Q. *Bioorg. Med. Chem. Lett.* **2011**, *21*, 5033−5036.

(6) McClure, D. S. *J. Chem. Phys.* **1954**, *22*, 1668−1675.

(7) (a) Jacobson, K.; Mouritsen, O. G.; Anderson, R. G. W. *Nat. Cell Biol.* **2007**, *9*, 7−14. (b) Kim, H. M.; Kim, B. R.; Choo, H.-J.; Ko, Y.-G.; Jeon, S.-J.; Kim, C. H.; Joo, T.; Cho, B. R. *ChemBioChem* **2008**, *9*, 2830−2838. (c) Kim, H. M.; Cho, B. R. *Acc. Chem. Res.* **2009**, *42*, 863−872.

(8) (a) Zheng, S. L.; Wang, Y.; Yu, Z.; Lin, Q.; Coppens, P. *J. Am. Chem. Soc.* **2009**, *131*, 18036−18037. (b) Bégué, D.; Qiao, G. G.; Wentrup, C. *J. Am. Chem. Soc.* **2012**, *134*, 5339−5350.

(9) Lee, J.; Kim, J.; Choi, W. *Environ. Sci. Technol.* **2007**, *41*, 5433−5438.

(10) See Table S1 (SI) for photophysical characterization including fluorescence turn-on ratios for all the pyrazolines.

(11) The following equation, $\delta_{cT} = \delta_{ur}C_rN_P/C_TN_r$, was used, where C_r and C_T are the initial concentrations of the reference compound (BHC-OAc) and tetrazole, respectively, N_P is the number of pyrazoline molecules formed per unit time, and N_r is the number of uncaged molecules per unit time. The literature value of the uncaging action cross-section of BHC-OAc, δ_{ur} = 0.95 GM, was used in the calculation. See Figure S9 (SI) for details.

(12) (a) Lee, Y. J.; Wu, B.; Raymond, J. E.; Zeng, Y.; Fang, X.; Wooley, K. L.; Liu, W. R. *ACS Chem. Biol.* **2013**, *8*, 1664−1670. (b) Li, F.; Zhang, H.; Sun, Y.; Pan, Y.; Zhou, J.; Wang, J. *Angew. Chem., Int. Ed.* **2013**, *52*, 9700−9704.

(13) While tetrazoles **5** and **6** show similar two photon cycloaddition cross-sections (4.0 GM for **5** and 3.8 GM for **6**), we selected tetrazole **6** in our in vivo studies because the pyrazoline cycloadduct derived from tetrazole **6** was found to be far more resistant to photobleaching in the fluorescence microscopic studies compared to the pyrazoline cycloadduct derived from tetrazole **5**.

(14) Yu, Z.; Ho, L. Y.; Lin, Q. *J. Am. Chem. Soc.* **2011**, *133*, 11912−11915.

(15) (a) Miller, M. L.; Roller, E. E.; Zhao, R. Y.; Leece, B. A.; Ab, O.; Baloglu, E.; Goldmacher, V. S.; Chari, R. V. J. *J. Med. Chem.* **2004**, *47*, 4802−4805. (b) Matesanz, R.; Rodríguez-Salarichs, J.; Pera, B.; Canales, A.; Andreu, J. M.; Jiménez-Barbero, J.; Bras, W.; Nogales, A.; Fang, W.-S.; Díaz, J. F. *Biophys. J.* **2011**, *101*, 2970−2980.

(16) Zhuang, Y. D.; Chiang, P. Y.; Wang, C. W.; Tan, K. T. *Angew. Chem., Int. Ed.* **2013**, *52*, 8124−8128.

(17) Tetrazole **6** and IPFAD showed no cytotoxicity toward CHO cells at concentrations ≤100 μM; see Figure S19 (SI) for details.

(18) The cytosolic fluorescence outside the rectangle boundary is due to rapid diffusion of the in situ generated nitrile imine intermediate within the cytosolic space of the individual irradiated cells.

(19) The decrease in fluorescence intensity after 43 s is due to photobleaching of the pyrazoline fluorophore at 405 nm excitation; see Figure S20 (SI) for details.

(20) Song, W.; Wang, Y.; Yu, Z.; Vera, C. I.; Qu, J.; Lin, Q. *ACS Chem. Biol.* **2010**, *5*, 875−885.

(21) The Pearson's correlation coefficient was determined to be 0.66. The reaction inside the cells was triggered by a hand-held 365 nm UV lamp because the subsequent fixation and immunostaining steps make it difficult to retrack the femtosecond 700 nm laser beam scanned area.

(22) Davis, M. J.; Kragor, C. H.; Reddie, K. G.; Wilson, H. C.; Zhu, Y.; Dore, T. M. *J. Org. Chem.* **2009**, *74*, 1721−1729.

(23) Yu, Z.; Pan, Y.; Wang, Z.; Wang, J.; Lin, Q. *Angew. Chem., Int. Ed.* **2012**, *51*, 10600−10604.

(24) Bianco, A.; Townsley, F. M.; Greiss, S.; Lang, K.; Chin, J. W. *Nat. Chem. Biol.* **2012**, *8*, 748−750.